Research Article

Sorption of Pt(IV) ions on poly(*m*-aminobenzoic acid) chelating polymer: Equilibrium, kinetic and thermodynamic studies

Tuğrul Öztürk[1] · **Mustafa Gülfen**[1] · **Abdil Özdemir**[1]

Received: 10 June 2020 / Accepted: 13 October 2020 / Published online: 26 October 2020

Abstract
In this work, poly(*m*-aminobenzoic acid) (PABA) chelating polymer was synthesized and its sorption behaviors for Pt(IV) ions have been investigated. The PABA polymer was prepared by the reaction of *m*-aminobenzoic acid with ammonium peroxydisulfate. Fourier transform-infrared spectroscopy (FT-IR), thermal analysis (TG and DTA), field emission-scanning electron microscopy (FE-SEM), energy dispersive spectroscopy (EDS), X-ray diffraction (XRD) and surface porosity analytical methods were used in the characterization of the polymer. The FE-SEM images showed that the particles of the synthesized PABA polymer were about 2–10 µm. The PABA polymer is thermally stable up to 320 °C. The zero charge point of the polymer was found at pH 3.50. Batch adsorption experiments were used to examine the effects of pH, initial Pt(IV) concentration, contact time and temperature. The best adsorption values were obtained at pH 4, in which is above the zero charge point of the polymer. The equilibrium, kinetics and thermodynamics of Pt(IV) adsorption on the PABA polymer were examined. The Pt(IV) maximum adsorption capacity of the polymer is 2362 µg/g. The adsorption kinetic data fitted best to pseudo-second order kinetic model. The calculations with intra-particle diffusion and the Elovich models showed that the adsorption was controlled by intra-particle diffusion and chemisorption. The adsorption data fitted well to the Langmuir isotherm. It was found that the adsorption followed the pseudo-second-order kinetic model. In the thermodynamic calculations, the Gibbs free energies ($\Delta G°$: (−10.98)–(−17.38) kJ/mol), the enthalpy ($\Delta H°$:70.07 kJ/mol) and the entropy ($\Delta S°$: 215.3 kJ/mol) change values of the adsorption were calculated. The column adsorption–desorption and reusability studies of the PABA polymer were also performed. The results showed that Pt(IV) sorption on the PABA polymer is endothermic and chemical adsorption process which is governed by both ionic interaction and chelating mechanisms.

Keywords Platinum(IV) ions · Pol(*m*-aminobenzoic acid) · Adsorption · Chelating polymer

1 Introduction

Platinum metal is one of expensive metals among the platinum group metals [1]. It is used in many industrial areas such as automotive catalysts, pharmaceuticals, electronics, medical devices, fuel cells, jewelry, telecommunication, petroleum and chemical industries. Platinum is used extensively as automotive catalysts which contain palladium, rhodium and platinum [2–4]. The production of platinum from primary ore resources or waste materials i.e. spent catalysts is important because of its high price [5, 6]. One of hydrometallurgical platinum production steps is selective recovery Pt(II) or Pt(IV) ions after the dissolution process of the wastes including other low price metal ions. During the dissolution processes, since oxidative reagents were used, Pt(IV) ion is favorable in the leaching solutions. Therefore, the recovery or separation of Pt(IV) ions from leach solutions is important. There are many adsorbents for the recovery of

✉ Mustafa Gülfen, mgulfen@sakarya.edu.tr | [1]Department of Chemistry, Faculty of Arts and Sciences, Sakarya University, 54187 Sakarya, Turkey.

Pt(IV) or Pt(II) ions from leach or waste solutions. Activated carbon [1, 7–9], silica [10, 11], ion exchangers [6], impregnate resins [12] chelating polymers [13, 14], biomass or natural polymers [15–17] have been used by different researchers. Adsorption methods are favorable in case of reusable adsorbents [18–26]. Activated carbon, ion exchangers, biomass, natural polymers shows sorption affinity to Pt(IV)/Pt(II) or other platinum group metal ions as well as other base metal ions (Cu(II), Pb(II) etc). Chelating polymers/resins or the adsorbents impregnated with a chelating group are preferred because of their more selectivity to precious metal ions than base metal ions [27]. The selectivity of chelating polymers corresponds to the Pearson's hard-soft acid-base (HSAB) theory which soft metal ions, for instance Pt(II), prefer to coordinate with soft bases (S > N > O) and hard metal ions, for Cu(II), to hard bases (O > N > S) [28].

In this study, poly(*m*-aminobenzoic acid) (PABA) chelating polymer was synthesized. PABA polymer is a conducting polymer with electron-rich nitrogen atoms and carbonyl groups [29, 30]. This polymer includes primary amine (–NH_2 as end group), secondary amine (>NH) and carboxylic acid (–COOH) chelating functional groups. Additionally, PABA polymer has the capabilities of ionic interaction/association of the protonated amine groups (–NH_3^+, >NH_2^+) with anionic metal ion complexes such as $PtCl_6^{2-}$ in the solution. The carboxyl acid groups can behave as ion exchanger group with cationic metal ions during the adsorption [28–30]. Poly(*m*-aminobenzoic acid) has been studied for different aims in earlier studies. However, there is no work about Pt(IV) adsorption onto poly(*m*-aminobenzoic acid) polymer, which constitutes the novelty of this study. Pt(IV) adsorbed poly(*m*-aminobenzoic acid) polymer together with amine and carboxylic acid functional groups and redox properties can be used as catalyst, solar cell material or any other application.

In the present work, the adsorption of Pt(IV) ions onto the synthesized PABA polymer has been investigated. The equilibrium, kinetics and thermodynamics of Pt(IV) ion adsorption were examined by varying the acidity of the solution, initial Pt(IV) concentration, contact time and temperature. The polymer was characterized by Fourier transform-infrared spectroscopy (FT-IR), thermogravimetric analysis (TG), differential thermal analysis (DTA) and field emission-scanning electron microscopy (FE-SEM) and energy dispersive spectroscopy (EDS).

2 Materials and methods

2.1 Materials

m-Aminobenzoic acid (mp: 178–180 °C, bp: 308 °C, 98%) was obtained from Sigma-Aldrich Chemie (GmbH, Steinheim, Germany). It was used in the polymerization without any further purification. The ammonium peroxydisulfate ($(NH_4)_2S_2O_8$) was obtained from Sigma-Aldrich Chemie (GmbH, Steinhem Germany). It was used as the oxidant of the polymerization. Pt(IV) standard solution for inductively coupled plasma-optical emission spectroscopy (ICP-OES) was purchased from Fluka (Steinhem, Germany). The concentration of the standard solution was 1000 mg/L Pt(IV) in 1 mol/L HCl. It was used in the preparing the desired concentrations for the adsorption studies and ICP-OES calibration measurements. In the preparation of the experimental solutions, ultrapure water (18.2 MΩ) was used and it was produced by Milli-Q (UK) ultrapure water (Type 1) system. All the other chemicals were in analytical grade.

2.2 Synthesis of poly(*m*-aminobenzoic acid)

Poly(*m*-aminobenzoic acid) (PABA) chelating polymer was obtained by using *m*-aminobenzoic acid monomer. *m*-Aminobenzoic acid was oxidized in the presence of ammonium peroxydisulfate (APS, $(NH_4)_2S_2O_8$) as similar to the polymerization of aniline.

The PABA synthesis reactions are demonstrated in Fig. 1 [29–32]. In the synthesis of the PABA polymer, 3.428 g (25 mmol) of *m*-aminobenzoic acid and 11.41 g (50 mmol) of APS were used to provide the molar ratio of the monomer to the oxidant as 1:2. Their solutions were prepared separately in 100 mL water. The obtained solutions were acidified by adding 2 mL HCl solution (36.5%). Both solutions were heated up to 50 °C temperature. The prepared APS solution was added dropwise into the *m*-aminobenzoic acid solution and meanwhile the mixture was stirred vigorously. Brownish black PABA polymer precipitate began to be seen after 5 min. The PABA synthesis reaction was continued by stirring the suspension at the temperature of 50 °C for 24 h. The obtained PABA polymer was filtered and washed with 0.1 M HCl solution and then ultrapure water. HCl washing provides the removal of HSO_4^- ions adsorbed on the polymer. HSO_4^- ions come from the ammonium peroxydisulfate as the oxidative reactant. HCl can be evaporated during the drying of the polymer, but HSO_4^- cannot be evaporated easily. The PABA polymer was dried in vacuum oven at 40 °C for 3 h [29–40]. The photo of the obtained PABA polymer powder is also given in Fig. 2. At these synthesis conditions of the PABA, about 64% yield was obtained. To produce more amount of the PABA, this synthesis procedure was repeated by using same amounts of the reagents and solvents. At the end of the synthesis, the PABA polymeric yield was calculated as about 64%. The obtained PABA polymer was used in the later experimental studies. By using same protocol,

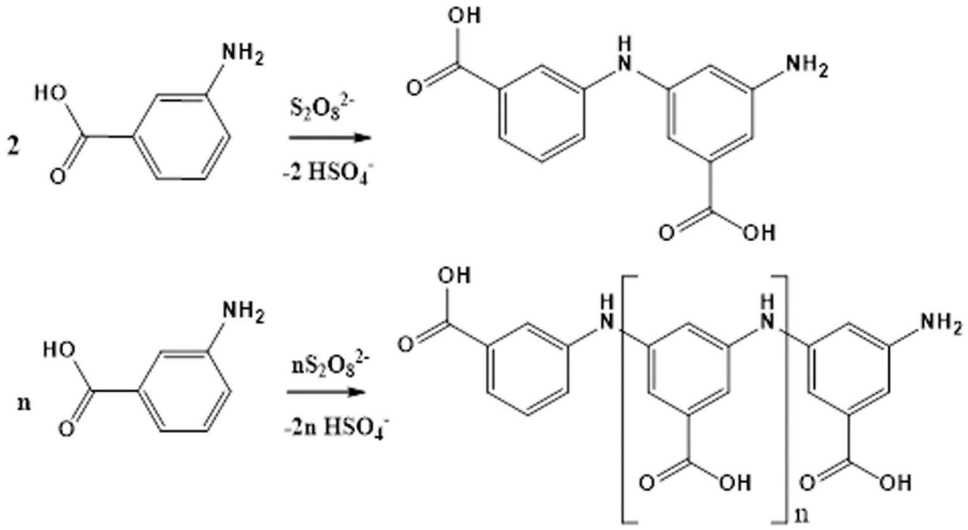

Fig. 1 Synthesis reaction of poly(*m*-aminobenzoic acid) chelating polymer

Fig. 2 Poly(*m*-aminobenzoic acid) chelating polymer (Brownish black powder)

polyaniline was also synthesized to compare with the PABA polymer.

2.3 FT-IR analysis

Fourier transform-infrared spectroscopy (FT-IR) was used to identify the functional groups in the prepared polymer and also to prove the adsorption of Pt(IV) ions. The FT-IR spectra of the *m*-aminobenzoic acid, the PABA and the Pt(IV) adsorbed PABA polymer samples were taken. Spectrum Two model FT-IR spectrometer (Perkin Elmer) equipped with ATR was used in the measurements which were recorded in the range of 400 and 4000 cm^{-1}. The *m*-aminobenzoic acid was measured without any purification. In the FT-IR measurements of the PABA, previously prepared polymer sample was used. For the FT-IR of the Pt(IV) adsorbed PABA, the sample was prepared by an adsorption equilibrating 1 g polymer in 100 mL 75 mg/L Pt(IV) solution at 25 °C for 24 h. The PtIV) adsorbed PABA polymer was filtered and washed with ultrapure water. Then it was dried in vacuum oven at 40 °C for 3 h.

2.4 Thermal analysis

The synthesized PABA chelating polymer was examined by using thermal analysis methods. At the same conditions, polyaniline (PANI) polymer was also synthesized and the thermal stability of the synthesized PABA polymer was examined together with the PANI. A Netzsch STA 449F1 model (GmbH, Geratebau, Germany) thermal analyzer device was used. Thermogravimetric (TG) and differential thermal analysis (DTA) curves of both the polymer samples were obtained. About 20 mg of the PABA and PANI polymer samples were used in the measurements. The TG and DTA curves were obtained by performing with the samples in the alumina crucible of the device at the temperatures from 25 °C to 800 °C, with a heating rate of 10 °C/min and under air atmosphere.

2.5 FE-SEM/EDS analyses

The surface morphology and particle structure of the PABA polymer were examined by using field emission-scanning electron microscopy (FE-SEM) equipped with energy dispersive X-ray spectroscopy (EDS). A Quanta™ 450 FEG model FE-SEM/EDS instrument (FEI Company, USA) was used in the measurements. The FE-SEM images of the PABA and the Pt(IV) adsorbed PABA polymer were taken at the conditions of 15.00 kV and 4.10×10^{-4} Pa pressure. The FE-SEM images were recorded at the different magnifications of 5000× and 20,000×. The surface elemental

distributions of the PABA polymer and the Pt(IV) adsorbed PABA polymer were determined by using the energy dispersive X-ray spectroscopy (EDS). The Pt(IV) adsorbed PABA polymer sample was prepared by equilibrating the 0.5 g polymer in 100 mL 75 mg/L Pt(IV) solution. The PABA and the Pt(IV) adsorbed PABA polymer samples were filtered, washed with ultrapure water and dried at the temperature of 100 °C.

2.6 X-ray diffraction analysis

The crystallinity of the PABA and Pt(IV) adsorbed PABA polymer samples were examined using a Rigaku Powder X-ray diffraction (XRD) system (Model D/MAX-2200 Ultima/PC (Japan), having CuKα source (λ = 0.154 nm). The XRD patterns were measured from 5° to 90° of 2θ angle. In the measurements, previously prepared PABA and Pt(IV) adsorbed polymer samples were used.

2.7 Surface area and porosity analysis

A Micromeritics TriStar II 3020 surface area and porosity analyzer (Micromeritics Co., US) was used to the surface area and porous properties of the PABA polymer performing N_2 adsorption–desorption method at 77.350 K temperature. Brunauer–Emmett–Teller (BET) and Langmuir surface areas were obtained from the adsorption–desorption data. Barrett–Joyner–Halenda (BJH) and Dollimore–Heal (D-H) adsorption-desorption pore sizes and the cumulative pore volumes were calculated using the software of the device. The samples were degassed at 473 K for 2 h before the measurements.

2.8 Adsorption studies of Pt(IV) ions

2.8.1 Effect of pH

The adsorption of Pt(IV) ions by the PABA polymer was studied at different acidic conditions to examine the effect of acidity on the adsorption. The experimental adsorption studies were performed with 100 mL of 30 mg/L Pt(IV) solutions at the different acidities of pH 0–6, by equilibrating with 0.7 g PABA polymer for 25 h. The pHs of the Pt(IV) solutions were adjusted using HCl or NaOH solutions. The experiments were carried out on magnetic stirrers at 25 °C during the adsorption period. 2 mL-sample solutions were taken in determined time intervals for the determination of the Pt(IV) ions in the solution phase. The Pt(IV) ion concentrations in the solution phases were determined before the adsorption and at the determined time intervals by using inductive couple plasma-optic emission spectrometer (ICP-OES). Percent adsorption values of Pt(IV) ions at the different acidic conditions were calculated. In addition, 1 g of the PABA polymer was titrated with 0.05 M NaOH solution. The polymer sample was equilibrated in 100 mL 1 M HCl solution. Then the polymer was filtered and washed with ultrapure water. 1 g polymer was added into 100 mL ultrapure water and potentiometric acid–base titration was performed. pH values were noted during the titration.

2.8.2 Effect of initial Pt(IV) concentration

The effect of initial Pt(IV) concentration on the adsorption was studied. For this aim, serial solutions at the different Pt(IV) concentrations of 10, 15, 20, 30 and 40 mg/L were prepared by keeping the solution pH constant at 4 as the optimum acidity, which had been determined before. The adsorption experiments were carried out by using 0.8 g PABA polymer in 100 mL Pt(IV) solutions at temperature of 25 °C for 26 h. The samples were taken in determined contact time intervals and their Pt(IV) ion concentrations were analyzed by using ICP-OES. From residual Pt(IV) concentrations, the adsorbed Pt(IV) amounts were calculated per g PABA polymer. The adsorption data were applied to the Langmuir and Freundlich isotherm models, and pseudo-first and pseudo-second kinetic models.

2.8.3 Effect of temperature

The effect of temperature on the Pt(IV) adsorption was studied at the temperatures of 20, 30, 40 and 50 °C. 1 g-polymer samples were equilibrated in 100 mL 20 mg/L Pt(IV) solutions at pH 4 for 26 h. The sample solutions were taken at the determined time intervals and the residual Pt(IV) ion concentrations were determined by using ICP-OES. The amounts of adsorbed Pt(IV) ions on the PABA polymer were calculated for each temperature. The appeared dispersion equilibrium constants (K_d), for the Pt(IV) adsorption at different temperatures were calculated from the ratio of the adsorbed Pt(IV) concentration, C_a *to* the solution equilibrium Pt(IV) concentration, C_e. The obtained K_d values were used in the calculations of the thermodynamic parameters of Gibbs free energy ($\Delta G°$) enthalpy ($\Delta H°$) and entropy ($\Delta S°$) changes for the Pt(IV) adsorption.

2.8.4 Column studies and reusability

The reusability of the PABA polymer for the Pt(IV) adsorption was performed with continuous-flow adsorption-elution cycle experiments in a glass column which has the length of 15 cm and inner diameter of 0.8 cm. The column was filled with the PABA polymer to be the bed high of 2 cm. The constant flows of the adsorption and elution were provided with a peristaltic pump. Glass wool was placed as about 0.5 cm high at the bottom and the

top of the PABA polymer in the column. For the column adsorption experiments, 30 mg/L Pt(IV) ion solution adjusted pH 4 was passed through the column at flow rate of 0.5 mL/min. Each 10 mL of the effluent solution was collected separately and the Pt(IV) ion concentrations of them were determined using ICP-OES. Then, the column was washed by flowing distilled water. The elution of Pt(IV) ions was performed using the mixture solution including 1 M thiourea and 1 M HCl. The Pt(IV) concentrations in each collected effluent solutions of 10 mL were determined using ICP-OES. Three adsorption–elution cycles of the column studies were done to examine the reusability of the PABA polymer.

2.8.5 ICP-OES analysis

In this study, a Spectro Arcos model inductively coupled plasma-optical emission spectroscopy (ICP-OES) instrument (Spectro Analytical Instruments, Kleve, Germany) was used in the determination of Pt(IV) ion concentrations. It was equipped with a torch having radial viewing (Quartz, fixed, 3.0-mm injector tube) and an auto sampler. The operating conditions of the ICP-OES instrument were selected as radio frequency power of 1450 W, coolant plasma gas flow of 13.5 L/min, auxiliary gas flow of 1.0 L/min, nebulizer flow of 0.8 L/min, sample aspiration rate of 2.0 mL/min and polychromator temperature of 15 °C. The measurements were done as three replications, and the read time was 60 s for each replicate. The Pt(IV) ion concentrations were determined by the optical emission at the wavelength of 214.423 nm. The standard solutions of 100, 250, 500, 1000, 2000, 3000 and 4000 µg/L Pt(IV) were used for the calibration curve of the measurements. The calibration standard solutions were prepared by diluting a stock solution of 1000 mg/L Pt(IV) in 1 mol/L HCl. The limit of detection (LOD: $x_{bl} \pm 3$ s) of the calibration curve was determined as 15 µg/L Pt(IV).

3 Results and discussion

3.1 FTIR spectroscopy

The FT-IR spectra of *m*-aminobenzoic acid (ABA) monomer, poly(*m*-aminobenzoic acid) (PABA) polymer and the Pt(IV) adsorbed PABA polymer are given in Fig. 3. In FT-IR spectra, the peaks at 1560 cm^{-1} for amino benzoic acid monomer and at 1575 cm^{-1} for poly(amino benzoic acid) polymer are assigned to the C–C ring stretching vibrations of the benzenoid ring. The C=O stretching peak at 1693 cm^{-1} and the O-H stretching peak at 2964 cm^{-1} confirm the presence of carboxylic acid functional group. Specific primary amine peaks between 3000 and 3500 cm^{-1} for *m*-aminobenzoic acid monomer were not observed. This is due to the hydrogen bonding between amino and carboxylic acid groups. The peaks at 3060 and 3218 cm^{-1} of the PABA polymer were assigned for secondary amine peaks. Also, the peaks between 1580 and 1490 cm^{-1} are typical secondary amine peaks of PABA polymer. The band observed in the spectra of the polymer at 754 cm^{-1} corresponds to the C–H out-of-plane bending vibration of the substituted benzene ring [31, 35, 40–42]. The peak at about 1189 cm^{-1} wavenumber belongs to the benzenoid C–N bonds of the polymer. After Pt(IV) adsorption, this peak shifted to1192 cm^{-1}. This shows that Pt(IV) ions were bound via chelating mechanism ($Pt(IV)_{+++}NH<$). The FT-IR results confirmed the polymerization reaction proceeded by bonding C–NH–C between *m*-aminobenzoic acid monomer molecules. Pt(IV) ions were bound to the polymer via chelating mechanism ($>NH_{+++}PtCl_5^-$). The shoulder of the broad peak of the protonated amines changed from 3067 to 3062 cm^{-1}. This may be due to the binding of PtIV) ions to protonated amines *via* ionic interaction ($>NH_2^+PtCl_6^{2-}$). Both chelating and ionic interaction mechanisms are possible in the adsorption.

3.2 Thermal analysis

The thermal stability and degradation of the PABA polymer was examined by using thermal analysis methods. During the synthesis of the polymer, polyaniline (PANI) polymer was also synthesis to compare with each other. Poly(*m*-aminobenzoic acid) polymer is a substituted polyaniline and their polymerizations have similar oxidation mechanism with APS. The obtained thermogravimetric (TG) and differential thermal analysis (DTA) curves of the PABA and PANI polymers are given in Fig. 4a and b. According to the TG curve of the PABA polymer, it was found that the PABA showed high thermal stability from room temperature to about 320 °C temperature (Fig. 4a). The PANI polymer is stable up to 315 °C (Fig. 4b). The PABA and PANI polymers showed relatively small weight loss 100–300 °C due to probably water and HCl releasing. The PABA polymer started to decompose above 320 °C temperature and the PANI was above 315 °C. The DTA curve of the PABA polymer also confirms that the polymer starts to decompose above 320 °C. The melting point of *m*-aminobenzoic acid monomer is 180 °C and the boiling point is 308 °C. The fact that there is no considerable endothermic peak at 180 °C is that the polymerization was confirmed and there is no monomer molecule which had not polymerized. In addition, the DTA curves of the both polymer show that there is no any glass transition and melting points. The thermal analysis also revealed that the PABA polymer will be used as an adsorbent for high temperatures as well.

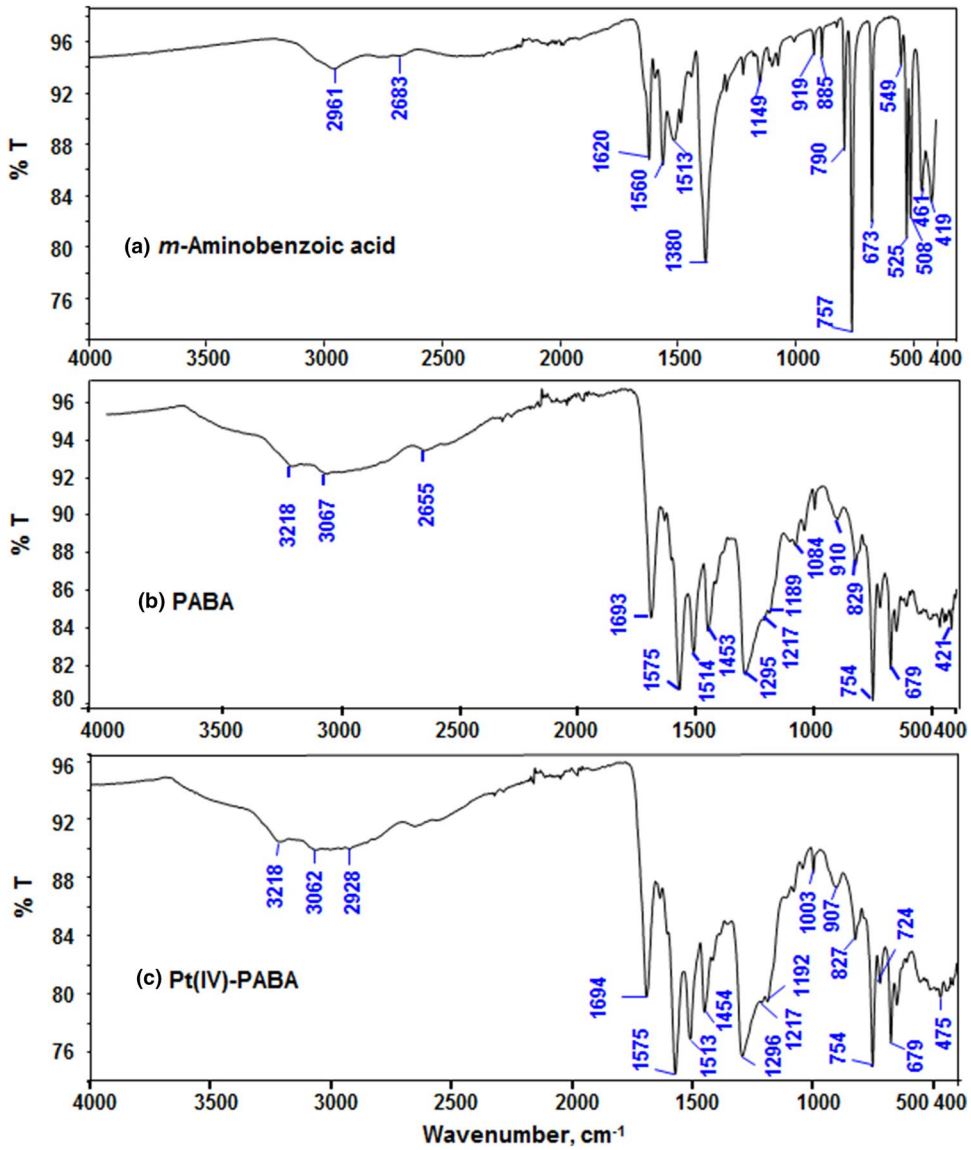

Fig. 3 FT-IR spectra of (**a**) *m*-aminobenzoic acid, (**b**) PABA polymer and (**c**) Pt(IV) adsorbed PABA

3.3 FE-SEM/EDS analysis

The synthesized PABA and the Pt(IV) adsorbed PABA polymer samples were examined by doing FE-SEM and EDS analyses. The obtained FE-SEM images of the PABA and Pt(IV) adsorbed PABA are given in Figs. 5 and 6, respectively. The FE-SEM images are recorded at different magnifications of 5000× and 20,000×. According to the FE-SEM images, it was observed that the PABA polymer particles have about 2–10 µm particle size. The polymer particles seem as melted and sintered globular microparticles (Fig. 5). The PABA polymer has a rugged surface and some cavities in its surface structure that are favorable for the uptake of Pt(IV) ions. After the adsorption of Pt(IV) ions, new accumulations on the polymer microparticles were observed (Fig. 6). Moreover, the elemental analyses of the PABA and the Pt(IV) adsorbed PABA polymer samples were done by EDS method. The obtained EDS results are given in Fig. 7. The atomic numbers of C, N and O elements on the surface of the PABA were found as about 66, 11 and 24, respectively (Fig. 7a). *m*-aminobenzoic acid monomer molecule includes 7 C, 1 N and 2 O atoms. The EDS analysis confirms nearly the chemical composition of the PABA polymer. In addition, 1.24% Cl content as low quantity of the Cl^- ions shows that the PABA polymer was washed well. After the adsorption of Pt(IV) ions, it was found that the PABA polymer includes about 0.04% Pt (Fig. 7b). This result confirms the adsorption of Pt(IV) ions on the PABA polymer.

3.4 X-ray diffraction analysis

The crystallinity of PABA polymer and Pt(IV) adsorbed PABA polymer samples were examined using X-ray

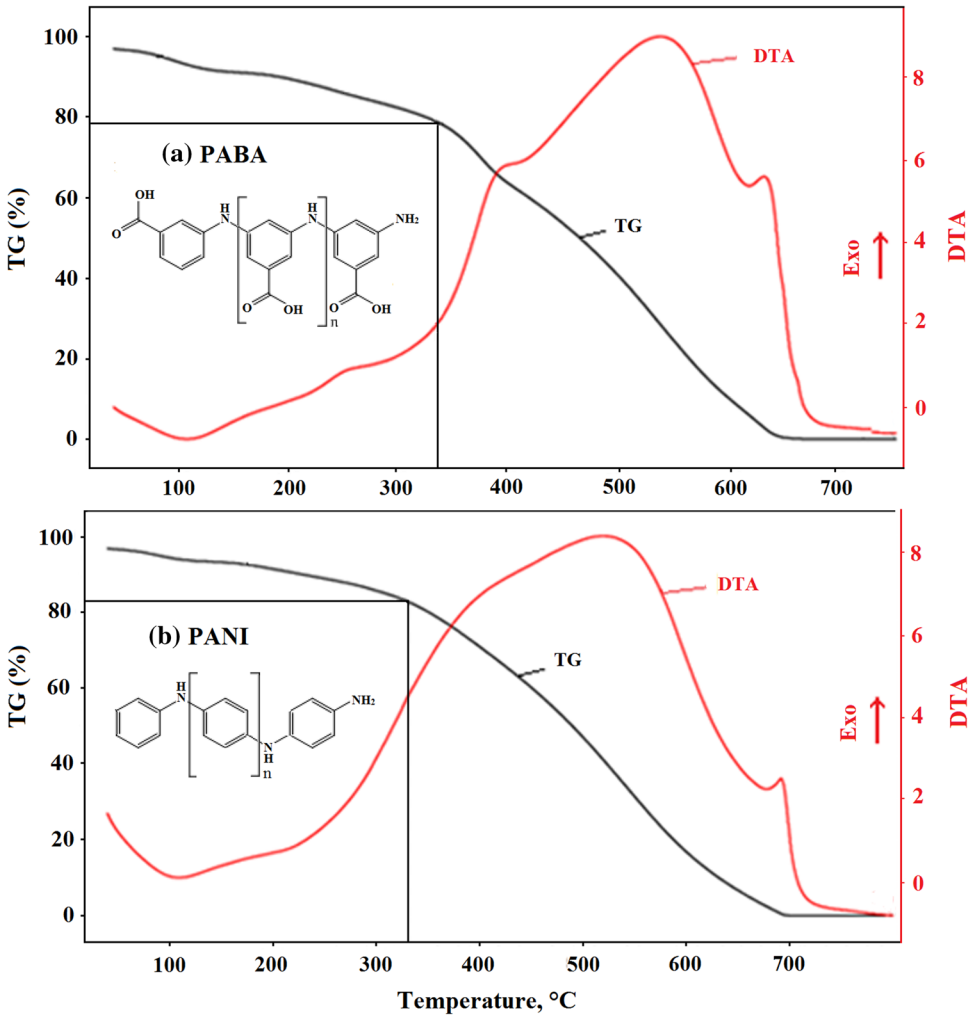

Fig. 4 TG and DTA analyses of (**a**) poly(*m*-aminobenzoic acid) (PABA) and (**b**) polyaniline (PANI)

diffraction (XRD) method. The obtained XRD patterns are given in Fig. 8. In the XRD patterns, significant crystal peaks were assigned as 12.5°, 17.2°, 25.2° and 27.9° for the PABA and 12.9°, 17.1°, 25.1° and 27.9° for the Pt(IV) adsorbed PABA polymer. It was found that the PABA polymer has high crystallinity properties with these high intensity peaks. Same XRD patterns were observed for the PABA polymer before and after Pt(IV) ion adsorption. After the Pt(IV) ion adsorption, metallic Pt peaks were not detected. This means that Pt(IV) ions does not reduce to metallic Pt during the adsorption.

3.5 Surface area and porosity

The surface area and porous properties of the PABA polymer were performed with N_2 adsorption–desorption method at 77.350 K temperature. Brunauer–Emmett–Teller (BET) and Langmuir surface areas, and Barrett–Joyner–Halenda (BJH) and Dollimore–Heal (D–H) adsorption–desorption pore sizes and cumulative pore volumes were obtained from the adsorption–desorption data. It was found that the PABA polymer has the Langmuir surface area of 22.78 m^2/g and the BET surface areas of 14.35 m^2/g. The pore sizes of the polymer were obtained as 55.109 Å and 72.446 Å from the Barrett, Joyner and Halenda (BJH) adsorption and desorption (4 V/A) methods, and as 58.953 Å and 77.464 Å from the Dollimore–Heal (D–H) adsorption and desorption (4 V/A) methods, respectively. BJH adsorption cumulative volume of the pores between 17 Å and 3.000 Å width was found as 0.019999 cm^3/g. BJH desorption cumulative volume of the pores between 17 Å and 3.000 Å width was 0.028266 cm^3/g. It was found that the synthesized PABA polymer is a mesoporous material between 20 Å and 500 Å pore sizes identified by IUPAC [43].

3.6 Adsorption studies of Pt(IV) ions

3.6.1 Effect of pH

The pH of aqueous solutions in adsorption processes is an important parameter that influences both the metal ion

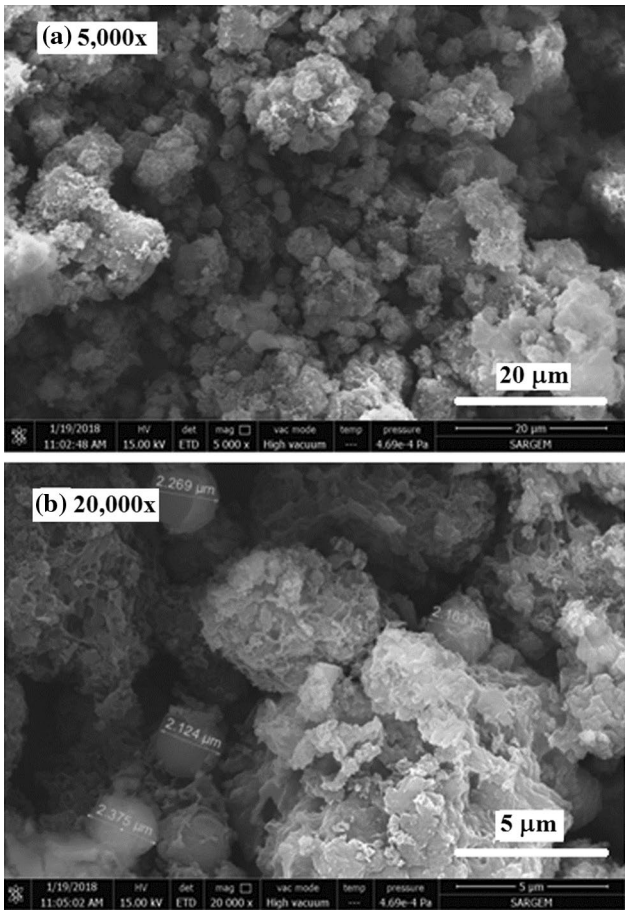

Fig. 5 FE-SEM images of PABA polymer at various magnifications (**a**) 5000× magnification and (**b**) 20,000× magnification

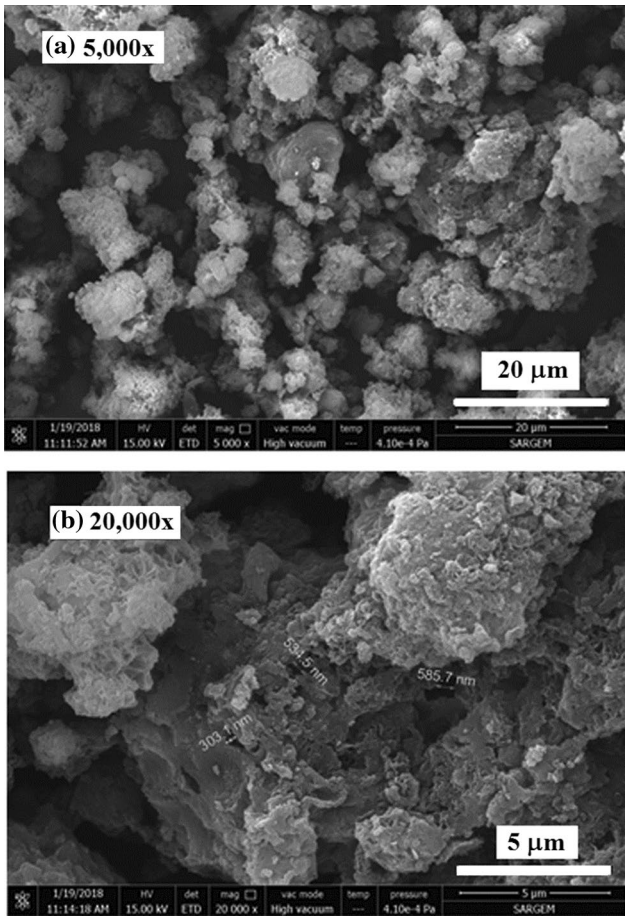

Fig. 6 FE-SEM images of Pt(IV) adsorbed PABA polymer at various magnifications (**a**) 5000× magnification and (**b**) 20,000× magnification

speciation in the solution phase and the surface chemistry of the adsorbents [44]. The species of Pt(IV) ions and the surface chemistry of the PABA polymer may change with related to the acidity of the solution. Therefore, the effect of acidity on Pt(IV) adsorption onto the PABA polymer was firstly studied in the range of pH 0–6. The adsorption percentage of Pt(IV) ions (S%) was calculated by using Eq. 1 and the adsorption results obtained at different acidic conditions are given in Fig. 9.

$$\text{Adsorption}\ (\%) = \frac{\left(C_i - C_e\right) \cdot 100}{C_i} \quad (1)$$

where, C_i and C_e are the initial and equilibrium concentrations of Pt(IV) in the solution (mg/L) before and after sorption, respectively.

It was observed from the acidity studies that the adsorption capacity varied noticeably by the solution acidity. At high acidic conditions below pH 4, lower adsorption ratios of Pt(IV) ions were obtained. There is a competitive adsorption between Pt(IV) and the available H^+ ions for the adsorbent at these acidic conditions. Therefore, low Pt(IV) adsorption values were observed at high H^+ ion concentrations. Higher adsorption ratios were observed at the pHs of 4–6. Pt(IV) ions form anionic chloro $[PtCl_6]^{2-}$ or hydroxy chloro $[Pt(OH)_nCl_m]^{2-}$ complexes with related to the pH and chloride concentration in the solution [28, 30]. Before the adsorption tests, NaCl was added to provide enough chloride concentrations for $[PtCl_6]^{2-}$.

On the other hand, the PABA polymer has protonation capability. Therefore, potentiometric acid–base titration was applied to the polymer. The obtained potentiometric acid–base titration curve is given in Fig. 10. It was observed that the PABA polymer has two equivalent points as about pH 3.50 and 8.50. Below pH 3.50 the polymer includes protonated amines ($>NH_2^+$ and $-NH_3^+$) and carboxylic acid (–COOH). At pH 3.50, the polymer has zero charge structure as deprotonated amines (>NH and $-NH_2$) and carboxylic acid (–COOH). The point of zero charge (pH_{zpc}) is the pH in which the surface of the adsorbent becomes neutral [19]. Above pH 8.50, the polymer converts to

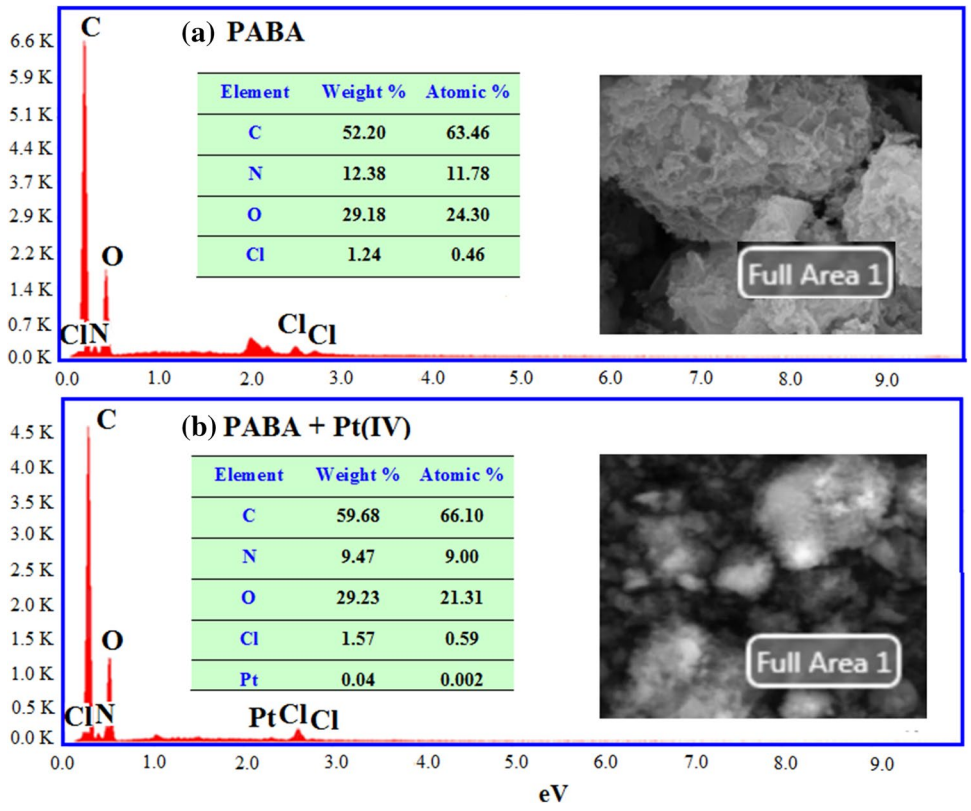

Fig. 7 EDS analyses of (**a**) PABA polymer and (**b**) Pt(IV) adsorbed PABA polymer

anionic form as carboxylate functional groups ($-COO^-$). H^+ ion exchange capacity of the polymer was found about 0.16 meq H^+/ g polymer. This H^+ exchange capacity is for solid surface of the polymer.

In case of considering the mechanism of the adsorption, ionic interaction and chelating mechanisms are possible during the adsorption of $[PtCl_6]^{2-}$ complex ions. For the adsorption of Pt(IV) ions on the PABA polymer, possible protonation of the polymer, ionic interaction and chelating reactions are given by Eqs. (2)–(7) [28, 30]. In addition, the ionic interaction and chelating mechanisms by considering the cationic, zero-charge and anionic forms of the PABA polymer are also shown in Fig. 11.

$$\text{R-NH-R} + H^+ + Cl^- \rightarrow \text{R-NH}_2{}^+\text{-R} + Cl^-(\text{Protonation}) \quad (2)$$

$$\text{R-COOH} + H^+ + Cl^- \rightarrow \text{R-COOH}_2{}^+ + Cl^-(\text{Protonation}) \quad (3)$$

$$2(R_2)NH_2{}^+ + [PtCl_6]^{2-} \rightarrow [(R_2)NH_2]_2{}^+[PtCl_6]^{2-}(\text{Ionic interaction}) \quad (4)$$

$$\text{R-COOH}_2{}^+ + [PtCl_6]^{2-} \rightarrow \text{R-COOH}_2{}^+[PtCl_6]^{2-}(\text{Ionic interaction}) \quad (5)$$

$$(R_2)NH_2{}^+ + [PtCl_6]^{2-} \rightarrow (R_2)NH_{++++}[PtCl_5]^- + H^+ + Cl^-(\text{Chelating}) \quad (6)$$

$$(R)(OH)C = O + [PtCl_6]^{2-} \rightarrow (R)(OH)C = O_{+++}[PtCl_5]^- + H^+ + Cl^-(\text{Chelating}) \quad (7)$$

By considering the adsorption mechanism reactions, the ionic interaction (Eqs. 4 and 5) requires high acidity and it occurs at below pH 3.50. The chelating mechanism (Eqs. 6 and 7) reveals H^+ ions, and this mechanism occurs at higher pH values than pH 3.50. The obtained results from the acidity studies showed that high adsorption ratio observed at pH 4–6. This pH range is above the zero charge point (pH: 3.50) of the PABA polymer. This means that the chelating mechanism is more effective in the adsorption. The ionic interaction also contributed the adsorption because of the adsorption capacities at high acidic conditions (pH 0 and 1). The pI of the PABA polymer was found at pH 3.5. The maximum adsorption capacity was obtained at pH 4. The adsorption capacities at pH 5 and 6 are lower than that at pH 4. At pH 5 and 6, more H-bond interaction between deprotonated amine (>NH) and carboxylic acid (COOH) may occur. Therefore, the interactions between polymer-polymer particles may be possible and this can be resulted in bigger polymer particles and less surface of the polymer particles. Consequently, the adsorption capacity decreased at pH 5 and 6. It can be concluded that both the ionic interaction and the chelating mechanism are possible and the chelating is more effective in the

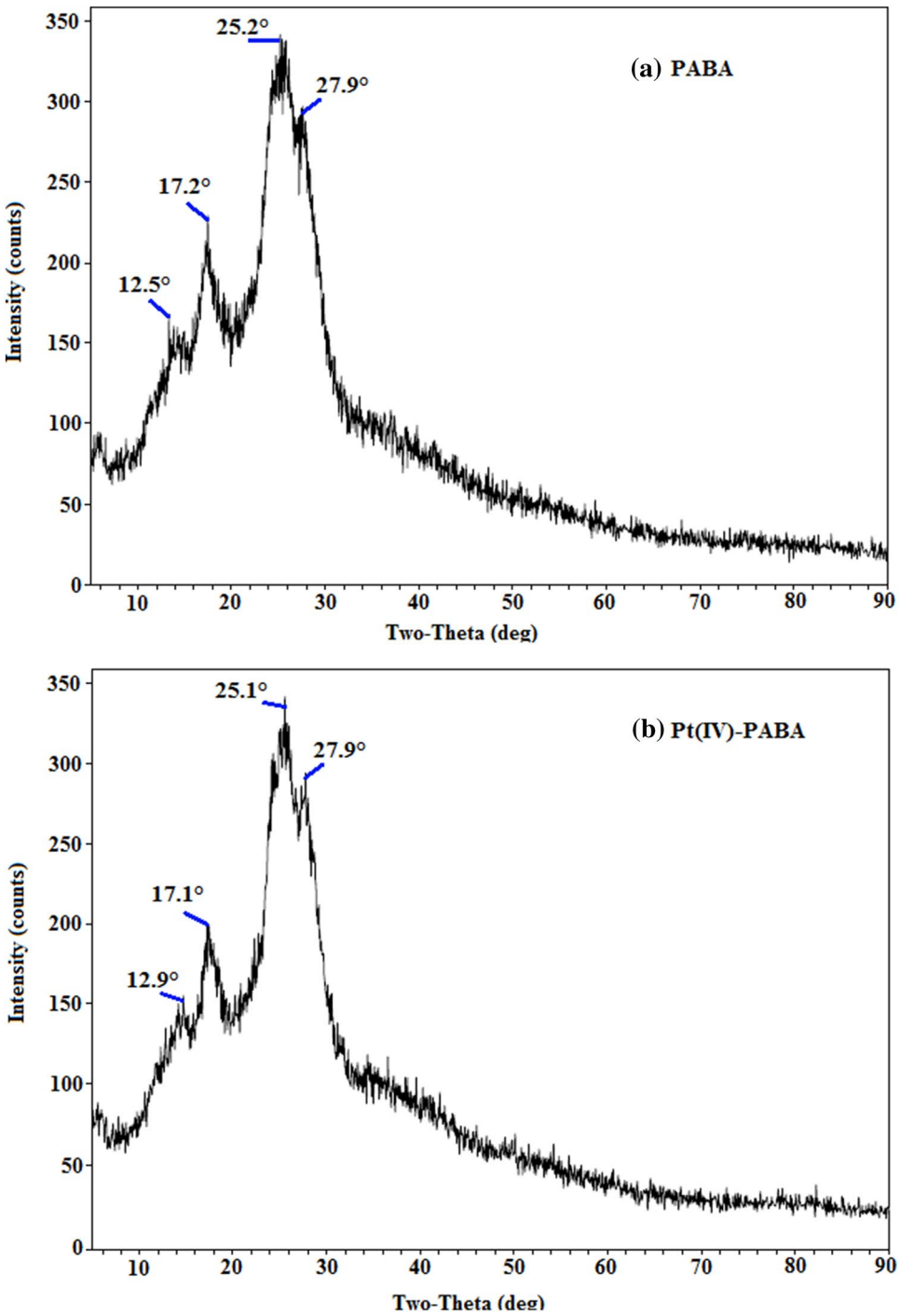

Fig. 8 XRD patterns of (**a**) PABA polymer and (**b**) Pt(IV) adsorbed polymer

adsorption of Pt(IV) ions. According to the results in Fig. 9, the optimum acidity of the solution was selected as pH 4 for the later Pt(IV) adsorption studies.

3.6.2 Adsorption isotherms

The adsorption tests were carried out with different initial concentrations of Pt(IV) ions, by keeping constant the acidity of the solutions at pH 4. The obtained adsorption results are given in Fig. 12. Adsorption isotherms are critical for the evaluation of any sorbent. The Langmuir

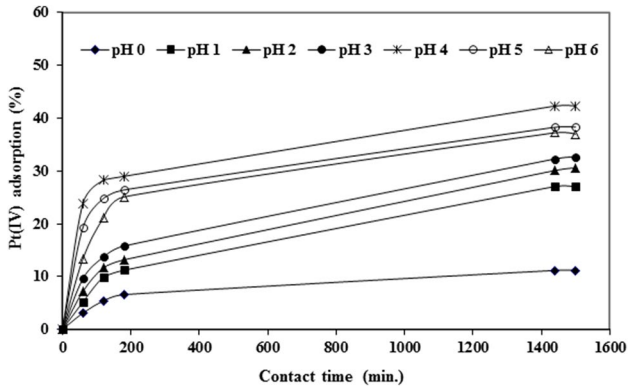

Fig. 9 Effect of initial pH on Pt(IV) adsorption (0.7 g polymer; 25 °C; 100 mL solution, 30 mg/L Pt(IV))

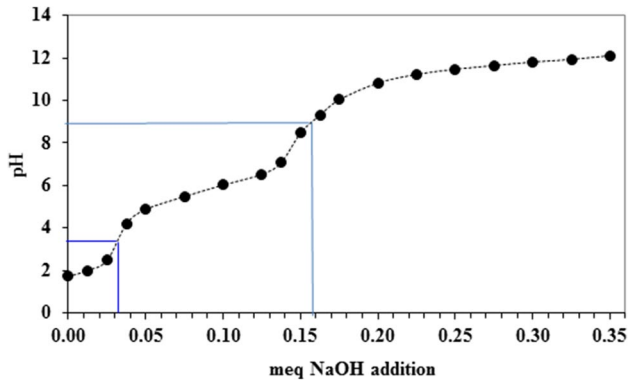

Fig. 10 Potentiometric acid–base titration of PABA polymer

and the Freundlich isotherm models were used to determine the relationship between the numbers of active site on the surface adsorption. The adsorption equilibrium data at different initial Pt(IV) concentrations were applied to the Langmuir and the Freundlich isotherm models.

The Langmuir isotherm model is based on monolayer adsorption on the active sites of the adsorbent on completely homogeneous surfaces. It assumes that the adsorbed layer is one molecule in thickness with chemical adsorption. The linearized equation of the Langmuir model is given by Eq. 8 [44–46].

The Freundlich isotherm model is based on adsorption on a heterogeneous surface and derived from the assumption that the adsorption sites are distributed exponentially with respect to the heat of adsorption. It indicates that the unequal size and shape of adsorbent surface is energetically responsible for the adsorption process and for multilayer adsorption. The logarithmic linear form of the Freundlich equation is given by Eq. 9 [44–47].

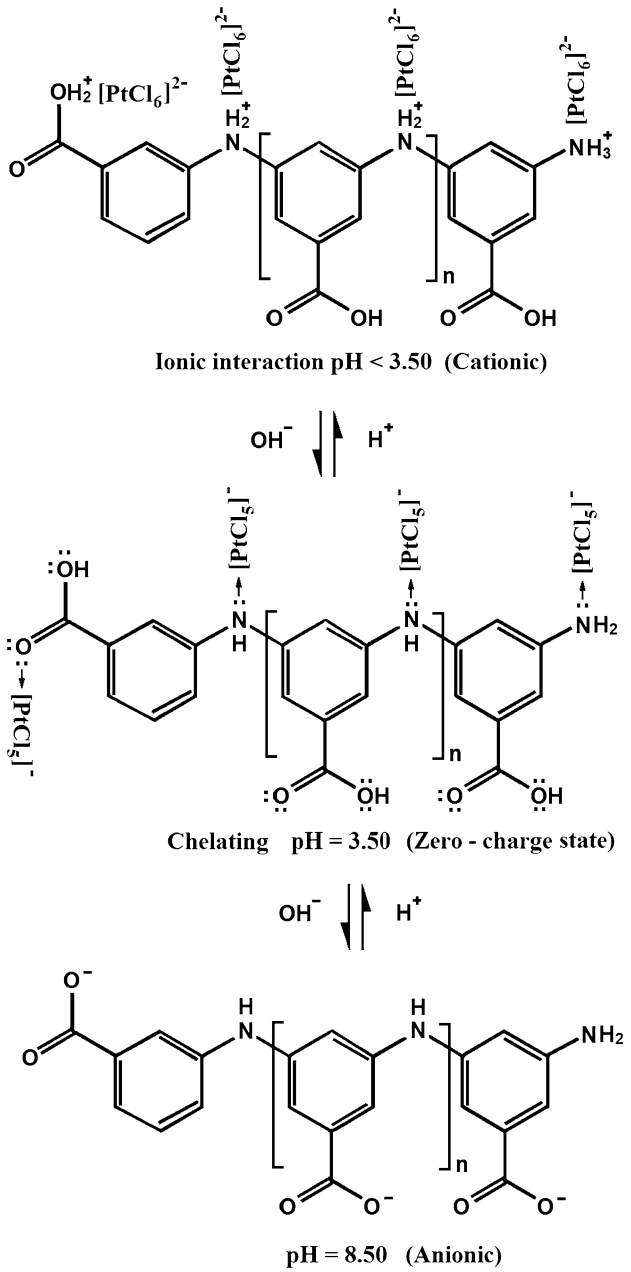

Fig. 11 Ionic interaction and chelating mechanisms and cationic, zero-charge and anionic forms of PABA polymer

$$\frac{C_e}{q_e} = \frac{C_e}{q_m} + \frac{1}{K_L q_m} \tag{8}$$

$$\ln q_e = \ln K_F + \frac{1}{n} \ln C_e \tag{9}$$

where, C_e (mg/L) is the equilibrium concentration of adsorbate; q_e (mg/g) is the amount of Pt(IV) ions adsorbed per gram of the adsorbent at the equilibrium; q_m (mg/g) is the maximum monolayer coverage capacity; K_L is the

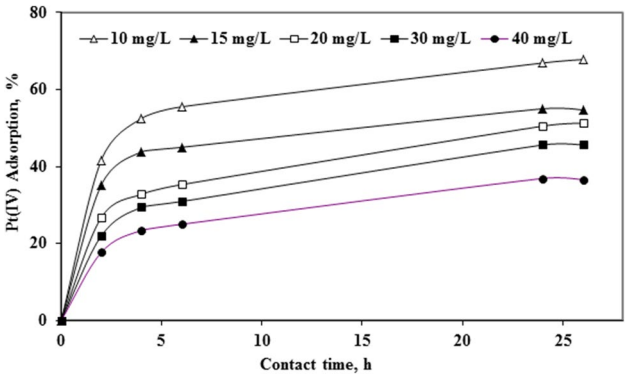

Fig. 12 Adsorption isotherms at different initial concentrations of Pt(IV) ions (0.8 g polymer; 25 °C; 100 mL solution, pH: 4)

Langmuir isotherm constant (L/mg); K_F is the Freundlich isotherm constant (mg/g) and n is the intensity (dimensionless) of the adsorbent.

The values of $1/n$ less than 1 represent a favorable adsorption [44–47].

The adsorption data were applied to the Langmuir and Freundlich isotherms by plotting the graphs of their linearized equations and the results are given in Fig. 13. The constants of both the isotherms were calculated and the obtained results are given in Table 1.

The regression coefficients were calculated as R^2: 0.9783 from the Langmuir isotherm and R^2: 0.9666 from the Freundlich isotherm. The regression coefficient from the Langmuir isotherm equation is higher than ones from the

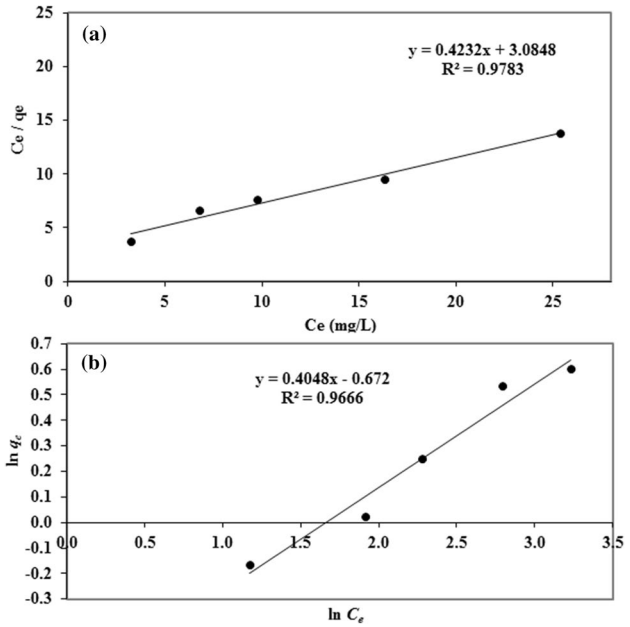

Fig. 13 (**a**) The Langmuir and (**b**) The Freundlich adsorption isotherms

Table 1 The constants of the Langmuir and the Freundlich isotherms

The Langmuir isotherm	R^2	q_m (µg/g)	K_L
	0.9783	2362	0.1372
The Freundlich isotherm	R^2	K_F (µg/g)	n
	0.9666	510.7	2.47

Freundlich equation. According to the regression coefficient values, it was found that the equilibrium adsorption data fitted better to the Langmuir isotherm than the Freundlich isotherm. The maximum Pt(IV) adsorption capacity of the PABA polymer was calculated as q_m: 2362 µg/g from the Langmuir isotherm. The Langmuir isotherm shows the monolayer adsorption with the energy homogeneity of the adsorption centers on the surface. Another assumption is that all the sites on the solid surface of an adsorbent are equal in size and shape which brings equal affinity for metal particles [47]. This also means that the Pt(IV) adsorption on the PABA polymer is a chemical adsorption process.

3.6.3 Adsorption kinetics

The pseudo-first-order and pseudo-second order kinetic models were tested to interpret the experimental Pt(IV) adsorption data. The linearized equations of the pseudo-first order and pseudo-second order kinetic models are given by Eqs. 10 and 11, respectively [48–50].

$$\ln\left(q_e - q_t\right) = \ln q_e - k_1 t \tag{10}$$

$$\frac{t}{q_t} = \frac{1}{k_2 {q_e}^2} + \frac{t}{q_e} \tag{11}$$

where, q_e and q_t (mg/g) are the amounts of Pt(IV) ions adsorbed per unit mass of the PABA polymer at equilibrium and time t (h), respectively, and k_1 (1/h) and k_2 (g/mg.h) the rate are constants of the pseudo-first-order and second-order adsorption, respectively. The experimental data were applied to the pseudo-first order and pseudo-second order kinetic models and the obtained linearized graphs are demonstrated in Fig. 14a and b. The q_e, k_1, k_2 and R^2 (Regression coefficients) values obtained from the kinetic model plots in Fig. 14 are also given in Table 2. It was found that the adsorption kinetics data were better represented by the pseudo-second-order kinetic model according to the obtained R^2 values. The pseudo-second order model depends on the supposition that the rate-limiting step could be chemisorption, with valence forces involved by electron exchange or sharing between the adsorbate and the adsorbent. The Pt(IV) adsorption is a

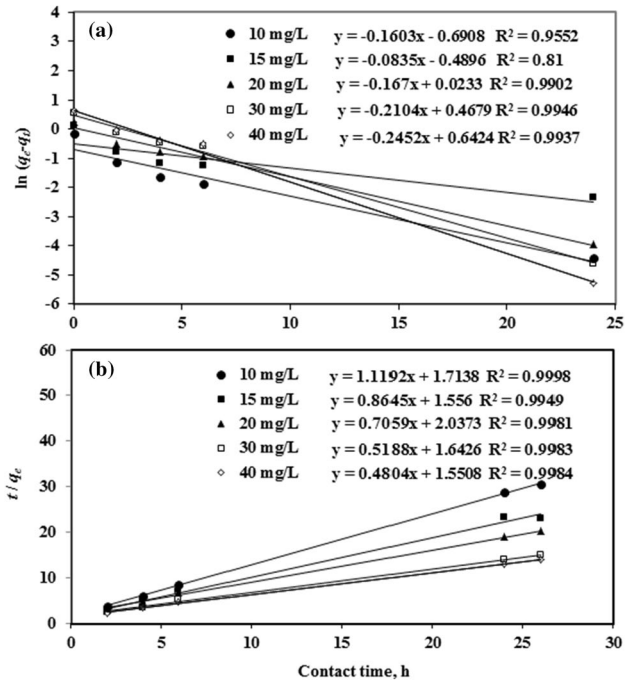

Fig. 14 (**a**) Pseudo-first order kinetic model and (**b**) Pseudo-second order kinetic model

chemisorption process which is the controlling step of the adsorption [51].

3.6.4 Adsorption mechanism

The adsorption mechanism of Pt(IV) ions on the PABA polymer was examined by applying the kinetic data to the intra-particle diffusion and the Elovich models. The intra-particle diffusion model developed by Weber and Morris is represented as following Eq. (12) The Elovich model equation is given as following Eq. (13) [51, 52]:

$$q_t = k_d t^{0.5} + \mathrm{C} \tag{12}$$

$$q_t = \frac{1}{\beta}\ln(\alpha\beta) + \frac{1}{\beta}\ln t \tag{13}$$

where k_d is the intra-particle rate constant ($g.mg^{-1}.h^{-0.5}$), and C is the intercept. The intra-particle diffusion model was applied by plotting q_t against $t^{0.5}$. α (mg g^{-1} h^{-1}) is the initial adsorption rate of the Elovich equation, and β ($g{\cdot}mg^{-1}$) is the desorption constant correlated to the extent of surface coverage and energy activation for chemisorption. The results obtained from the intra-particle diffusion and the Elovich model equations are given in Fig. 15a and b. In a solid–liquid adsorption, the adsorbate transfer occurs by either film diffusion, intra-particle diffusion or both [53]. The adsorption mechanism Pt(IV) ions onto the PABA polymer may occur by following steps during the adsorption; (1) The movement of Pt(IV) ions from the bulk solution to the external surface of the PABA polymer (Film diffusion). (2) The movement of Pt(IV) ions into the internals of the PABA polymer (Intra-particle diffusion). (3) The adsorption of Pt(IV) ions onto the interior pores of the PABA polymer (Adsorption) [51].

It can be seen from Fig. 15a that the plots of q_t versus $t^{0.5}$ are linear (R^2: 0.9199–0.9934). The intra-particle diffusion model predicts that the adsorption of Pt(IV) ions onto the PABA polymer is controlled by intra-particle diffusion [54]. C values (0.4692–0.6139) is the intercept points of the linear plots in Fig. 15a. They show the thickness of the film diffusion boundary layer in the adsorption process. The larger the value of C is, the thicker is the boundary layer. If the straight line passes through the origin, the intra-particle diffusion is the sole rate-determining step. Otherwise, other mechanisms may be involved. The Elovich equation has been widely used in adsorption kinetics, which describes chemical adsorption (chemical reaction) mechanism in nature [55–57]. The Elovich model for the adsorption of Pt(IV) ions onto the PABA polymer was carried out and the results are given in Fig. 15b. It can be noted from Fig. 15b that the linear fit curves exhibited the adaptability with the Elovich model. The adsorption can be described using the Elovich model. This outcome reveals that chemical adsorption between the active sites on the PABA polymer and Pt(IV) ions occurred.

Table 2 Parameters for pseudo-first order and pseudo-second order kinetic models

Initial concentration (Pt(IV) mg/L)	Pseudo-first order			Pseudo-second order		
	k_1	q_e	R^2	k_2	q_e	R^2
10	0.160	0.501	0.9552	1.085	0.893	0.9998
15	0.084	0.613	0.8100	0.713	1.157	0.9949
20	0.167	1.024	0.9902	0.363	1.417	0.9981
30	0.210	1.597	0.9946	0.243	1.928	0.9983
40	0.245	1.901	0.9937	0.221	2.082	0.9984

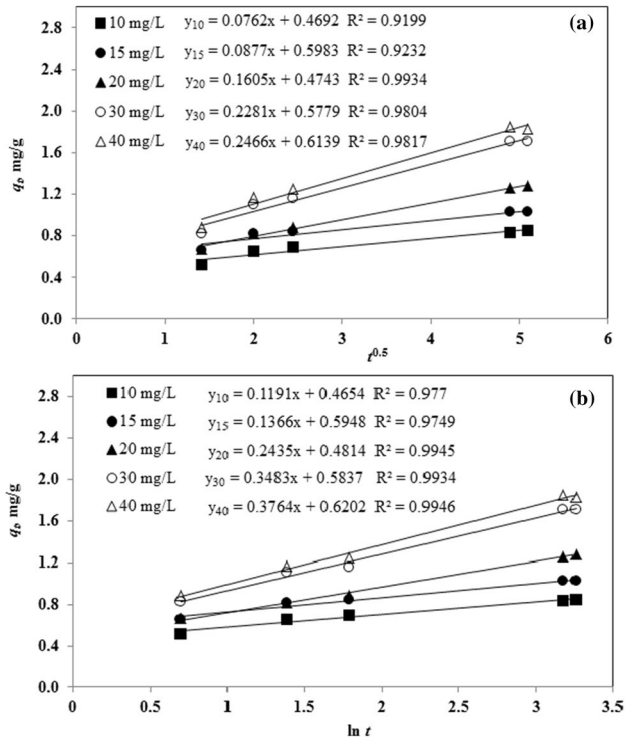

Fig. 15 (**a**) Intra-particle diffusion model, (**b**) Elovich model

3.6.5 Effect of temperature

The effect of temperature on the adsorption of Pt(IV) ions was studied at the temperatures of 20, 30, 40 and 50 °C. The adsorption results at different temperatures are given in Fig. 16. It was found that the adsorption capacity increased by increasing temperature. The increase at 50 °C temperature is higher than the other studied temperatures. These results show that the adsorption of Pt(IV) ions onto the PABA polymer is an endothermic process and favorable at high temperatures.

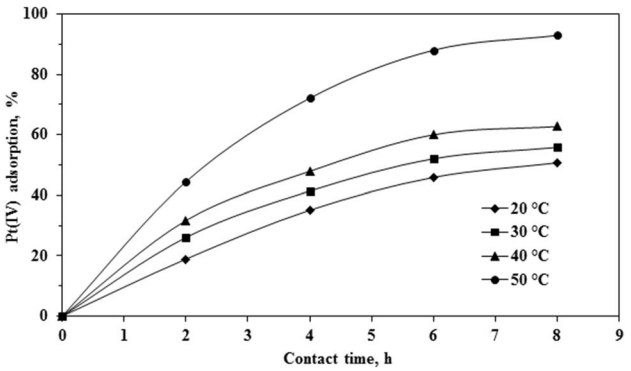

Fig. 16 Effect of temperature on the Pt(IV) adsorption

3.6.6 Adsorption thermodynamics

The thermodynamic parameters of the Pt(IV) adsorption in the studied experimental conditions were calculated to evaluate the spontaneity and the operability of the adsorption. Firstly, the appeared dispersion equilibrium constants, K_d were calculated from the ratios of the adsorbed Pt(IV) concentrations, C_a on the PABA polymer to the equilibrium Pt(IV) concentrations, C_e in the solution (Eq. 14). Then, the Gibbs free energy change ($\Delta G°$) values were obtained from the appeared K_d constants by using Eq. 15. The enthalpy ($\Delta H°$) and entropy ($\Delta S°$) changes were found from the slope and intercept by using the Van't Hoff equation (Eq.17) [58–61].

$$K_d = \frac{C_a}{C_e} \tag{14}$$

$$\Delta G° = -RT \ln K_d \tag{15}$$

$$\Delta G° = \Delta H° - T\Delta S° \tag{16}$$

$$\ln K_d = \frac{\Delta S°}{R} - \frac{\Delta H°}{RT} \tag{17}$$

where R is the gas constant, K_d is the dispersion equilibrium constant, T is the temperature (K), C_a is the equilibrium concentration of Pt(IV) on solid adsorbent (mg/kg), and C_e is the equilibrium concentration of Pt(IV) in the solution phase (mg/L).

The thermodynamic parameters within the studied experimental conditions were calculated for the PtIV) adsorption by applying to the Van't Hoff equation. The Van't Hoff linear plot of ln K_d versus 1/T obtained from the data is demonstrated in Fig. 17. The calculated thermodynamic parameters of $\Delta G°$, $\Delta H°$ and $\Delta S°$ are presented in Table 3. The negative values of $\Delta G°$ values (−10.98, −12.23, −13.68, −17.38 kJ/mol) were obtained and this indicates that the spontaneous nature of adsorption. The

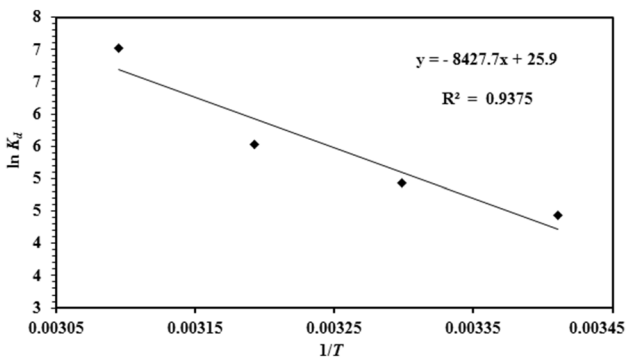

Fig. 17 The plot of ln K_d versus 1/T

Table 3 Thermodynamic parameters of Pt(IV) adsorption onto PABA polymer in the studied conditions

Temperature (°C)	$\Delta G°$ (kJ/mol)	$\Delta H°$ (kJ/mol)	$\Delta S°$ (J/mol)
20	−10.98	70.07	215.3
30	−12.23		
40	−13.68		
50	−17.38		

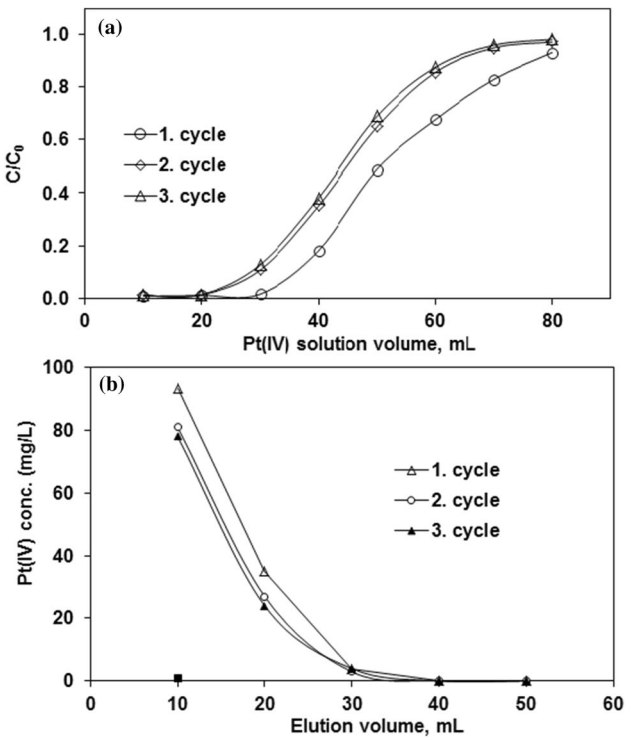

Fig. 18 Column (**a**) adsorption and (**b**) elution profiles

adsorption at higher temperatures is more favorable. The positive value of $\Delta H°$ (70.07 kJ/mol) confirms the endothermic nature of the adsorption. The $\Delta H°$ value which is higher than 40 kJ/mol, shows a chemisorption process. The positive $\Delta S°$ result shows the increase in the randomness at the solid/solute interface during the adsorption of Pt(IV) [59–61].

3.6.7 Column studies and reusability

Three adsorption and elution profiles of the column studies are given in Fig. 18a and b. After 30 mg/L Pt(IV) feed solution was adsorbed, 93 mg/L Pt(IV) elution solution was obtained at the end of first adsorption–elution cycle. This means that the Pt(IV) ions can be concentrated using the PABA polymer. Second and third cycles of the adsorption–elution were resulted in the adsorption and elution profiles with a small difference as lower than the first cycle. These results shows that the PABA polymer is a reusable adsorbent in the Pt(IV) adsorption.

3.7 Comparison with the results of Pt(II, IV) adsorption in literature

The comparison of the findings of Pt(IV) ion adsorption with some adsorption studies in the literature are given in Table 4. Wide range values of Pt(II,IV) adsorption capacities (q_m) were obtained in the literature. Because of platinum is high price metal, very low adsorption capacity may also be economic in the adsorption. There are adsorbents with lower adsorption capacity in the literature than the present study. In general, the Langmuir adsorption isotherm and pseudo-second order kinetics were found in the studies in the literature and same results were found in this study. Some researchers were found to be pH 0–2 for the acidity of the solution in the adsorption experiments with electrostatic interaction between the adsorbent and $PtCl_6^{2-}$ ions. However, it was found to be pH 4 for the optimum adsorption onto the PABA polymer with both ionic interaction and chelating mechanisms.

4 Conclusions

Poly(*m*-aminobenzoic acid) (PABA) chelating polymer has been synthesized and characterized. The adsorption of Pt(IV) ions onto the PABA polymer have been investigated. The thermal analysis results showed that the PABA polymer has high thermal stability up to about 300 °C temperatures. The particle sizes of the polymer were estimated at between 2 and 10 µm from FE-SEM images. The XRD results showed high crystalliniy of the polymer. The surface areas were determined as 22.78 m^2/g with the Langmuir model and of 14.35 m^2/g with the BET model. Mesoporous pore structure was detected on the polymer surface with 55.109–77.4644 Å obtained from BHJ and D-H methods. The adsorption of Pt(IV) ions onto the PABA polymer was found to be greatly dependent on the solution pH, contact time and temperature. From the pH studies, the optimum Pt(IV) adsorption was obtained at pH 4. The point of zero charge state of the PABA polymer was found about pH 3.50. The equilibrium studies showed that the adsorption data fitted better to the Langmuir isotherm than the Freundlich. The maximum Pt(IV) adsorption capacity of the PABA polymer was calculated as q_m: 2362 µg/g. The kinetics of the adsorption fitted better to the pseudo-second-order kinetic model which indicates the chemisorption process. Temperature is effective in the adsorption. Negative $\Delta G°$ values were obtained as −10.98, −12.23, −13.68

Table 4 Some adsorption studies of Pt(II,IV) ions in literature

Adsorbent-Functionality	Results	Ref.
Cr-based metal-organic frameworks (MIL101(Cr)-NH_2)	Langmuir isotherm. Pseudo-second order model. $PtCl_6^{2-}$-electrostatic attraction. pH 1.0. 24 h. q_m: 140.7 mg/g	[62]
Superparamagnetic Fe_3O_4@SiO_2-NH_2 nanoparticles	*Langmuir* isotherm. Pseudo-second order model. q_m: 12.5 mg/g	[63]
Biosorption on Fungi *Aspergillus* sp.	Langmuir isotherm. Pseudo-second order model. pH 2.0. 45 min. q_m: 5.49 mg/g	[64]
Magnetic cellulose hybrids anchored by quaternary amine moieties.	Langmuir and D-R adsorption isotherms. Pseudo-second order model. pH:2.0. q_m: 178 mg/g. $\Delta H°$: −18.7 kJ/mol	[65]
Polyethylenimine-aminated polyvinyl chloride fibers:	Langmuir isotherm. 0.1 M HCl. q_m: 410.53 mg/g	[66]
Hydrazine-functionalised zeolite	Langmuir isotherm. pH 2. 6 h. q_m: 0.117 mg/g	[67]
Lagerstroemia speciosa biomass modified by polyethylenimine	Langmuir isotherm Pseudo-second order kinetic model. Endothermic. Pt(II). pH 2 q_m: 122–154 mg/g	[68]
Polyethylenimine (PEI)/polyvinyl chloride (PVC)-crosslinked fiber	Langmuir.isotherm. q_m:217.31(mg/g). $\Delta H°$: 2.15 kJ/mol Endothermic	[59]
Magnetic cellulose functionalized with thiol and amine	Langmuir isotherm. q_m: 39.03 mg/g. pH: 2	[69]
Poly(*m*-aminobenzoic acid)	Langmuir isotherm. Pseudo-second order model. Ionic interaction and chelating mechanism. Endothermic. Chemisorption. q_m: 2362 µg/g. pH 4. 25 h	This study

and − 17.38 kJ/mol for 20, 30, 40 and 50 °C temperatures. The $\Delta H°$ value is calculated as 70.07 kJ/mol and $\Delta S°$ is 215.3 J/mol. The adsorption is spontaneous endothermic chemical sorption process. Intra-particle diffusion model is effective the Pt(IV) adsorption. The $\Delta H°$ value (> 40 kJ/mol) and the Evolich model confirmed the chemical sorption of Pt(IV) ions. Both ionic interaction and chelating mechanisms are included in the adsorption of Pt(IV) ions. Chelating mechanism is more effective. It was found from the adsorption–desorption cycles in the column studies that the PABA polymer is reusable adsorbent for Pt(IV) ions. In conclusion, poly(*m*-aminobenzoic acid) chelating polymer has Pt(IV) ion sorption capability and the Pt(IV) adsorbed PABA chelating polymer can be used in the applications of Pt(IV) recovery or solid catalysts.

Acknowledgements The authors are grateful for the financial support of the Commission of the Scientific Research Projects of Sakarya University (BAPK FBYL TEZ 2017-50-01-057).

Compliance with ethical standards

Conflict of interest The authors declare that they have no conflict of interest.

References

1. Wojnicki M, Socha RP, Luty-Błocho M, Fitzner K (2017) Kinetic studies of the removal of Pt (IV) chloride complex ions from acidic aqueous solutions using activated carbon. React Kinet Mech Catal 120(2):715–734. https://doi.org/10.1007/s11144-017-1151-9
2. Seymour RJ, O'Farrelly J, Potter LC (2000) Platinum-group metals. Kirk-Othmer encyclopedia of chemical technology. Wiley, New York. https://doi.org/10.1002/0471238961.1612012019052513.a01
3. Rao CRM, Reddi GS (2000) Platinum group metals (PGM); occurrence, use and recent trends in their determination. TRAC-Trend Anal Chem 19(9):565–586. https://doi.org/10.1016/S0165-9936(00)00031-5
4. Fontàs C, Salvadó V, Hidalgo M (2003) Selective enrichment of palladium from spent automotive catalysts by using a liquid membrane system. J Membr Sci 223(1–2):39–48. https://doi.org/10.1016/S0376-7388(03)00288-6
5. Nowottny C, Halwachs W, Schügerl K (1997) Recovery of platinum, palladium and rhodium from industrial process leaching solutions by reactive extraction. Sep Purif Technol 12(2):135–144. https://doi.org/10.1016/S1383-5866(97)00041-5
6. Peng L, Liu GF, Chen DL, Cheng SY, Ning T (2009) Adsorption properties of Ag(I), Au(III), Pd(II) and Pt(IV) ions on commercial 717 anion-exchange resin. Trans Nonferr Metal Soc China 19(6):1509–1513. https://doi.org/10.1016/S1003-6326(09)60061-3
7. Aktas S, Morcali MH (2011) Platinum recovery from dilute platinum solutions using activated carbon. Trans Nonferr Metal Soc China 21(11):2554–2558. https://doi.org/10.1016/S1003-6326(11)61091-1
8. Cox M, Pichugin AA, El-Shafey EI, Appleton Q (2005) Sorption of precious metals onto chemically prepared carbon from flax shive. Hydrometallurgy 78(1/2):137–144. https://doi.org/10.1016/j.hydromet.2004.12.006
9. Sharififard H, Zokaee Ashtiani F, Soleimani M (2013) Adsorption of palladium and platinum from aqueous solutions by chitosan and activated carbon coated with chitosan. Asia Pac J Chem Eng 8(3):384–395. https://doi.org/10.1002/apj.1671
10. Kang T, Park Y, Yi J (2004) Highly selective adsorption of Pt^{2+} and Pd^{2+} using thiol-functionalized mesoporous silica. Ind Eng Chem Res 43(6):1478–1484. https://doi.org/10.1021/ie030590k
11. Kramer J, Dhladhla NE, Koch KR (2006) Guanidinium functionalised silica-based anion exchangers significantly improve the selectivity of platinum group metal recovery from

process solutions. Sep Purif Technol 49(2):181–185. https://doi.org/10.1016/j.seppur.2005.09.004
12. Rovira M, Cortina JL, Arnaldos J, Sastre AM (1998) Recovery and separation of platinum group metals using impregnated resins containing Alamine 336. Solvent Extr Ion Exch 16:1279–1302. https://doi.org/10.1080/07360299808934580
13. Ni C, Yi C, Feng Z (2001) Studies of syntheses and adsorption properties of chelating resin from thiourea and formaldehyde. J Appl Polym Sci 82(13):3127–3132. https://doi.org/10.1002/app.2169
14. Park CI, Jeong JS, Cha GW (2000) Separation and preconcentration method for palladium, platinum and gold from some heavy metals using Amberlite IRC 718 chelating resin. Bull Korean Chem Soc 21(1):121–124. http://www.koreascience.or.kr/article/JAKO200013464474008.page
15. Abdel-Halim ES, Al-Deyab SS (2011) Removal of heavy metals from their aqueous solutions through adsorption onto natural polymers. Carbohydr Polym 84(1):454–458. https://doi.org/10.1016/j.carbpol.2010.12.001
16. Yoshikawa M, Ooi T, Izumi JI (1999) Alternative molecularly imprinted membranes from a derivative of natural polymer, cellulose acetate. J Appl Polym Sci 72(4):493–499. https://doi.org/10.1002/(SICI)1097-4628(19990425)72:4<493::AID-APP5>3.0.CO;2-U
17. Mack C, Wilhelmi B, Duncan JR, Burgess JE (2007) Biosorption of precious metals. Biotechnol Adv 25(1):264–271. https://doi.org/10.1016/j.biotechadv.2007.01.003
18. Gunasundari E (2017) Adsorption isotherm, kinetics and thermodynamic analysis of Cu(II) ions onto the dried algal biomass (Spirulina platensis). J Ind Eng Chem 56:129–144. https://doi.org/10.1016/j.jiec.2017.07.005
19. Kiruba UP, Kumar PS, Prabhakaran C, Aditya V (2014) Characteristics of thermodynamic, isotherm, kinetic, mechanism and design equations for the analysis of adsorption in Cd (II) ions-surface modified Eucalyptus seeds system. J Taiwan Inst Chem E 45(6):2957–2968. https://doi.org/10.1016/j.jtice.2014.08.016
20. Kumar PS, Ramalingam S, Abhinaya RV, Thiruvengadaravi KV, Baskaralingam P, Sivanesan S (2011) Lead (II) adsorption onto sulphuric acid treated cashew nut shell. Sep Sci Technol 46(15):2436–2449. https://doi.org/10.1080/01496395.2011.590174
21. Neeraj G, Krishnan S, Kumar PS, Shriaishvarya KR, Kumar VV (2016) Performance study on sequestration of copper ions from contaminated water using newly synthesized high effective chitosan coated magnetic nanoparticles. J Mol Liq 214:335–346. https://doi.org/10.1016/j.molliq.2015.11.051
22. Basha CA, Ramanathan K, Rajkumar R, Mahalakshmi M, Kumar PS (2008) Management of chromium plating rinsewater using electrochemical ion exchange. Ind Eng Chem Res 47(7):2279–2286. https://doi.org/10.1021/ie070163x
23. Vardhan KH, Kumar PS, Panda RC (2019) A review on heavy metal pollution, toxicity and remedial measures: current trends and future perspectives. J Mol Liq 290:111197. https://doi.org/10.1016/j.molliq.2019.111197
24. Muthusaravanan S, Sivarajasekar N, Vivek JS, Paramasivan T, Naushad M, Prakashmaran J, Gayathri V, Al-Duaij OK (2018) Phytoremediation of heavy metals: mechanisms, methods and enhancements. Environ Chem Lett 16:1339–1359. https://doi.org/10.1007/s10311-018-0762-3
25. Faisal AA, Al-Wakel SF, Assi HA, Naji LA, Naushad M (2020) Waterworks sludge-filter sand permeable reactive barrier for removal of toxic lead ions from contaminated groundwater. J Water Process Eng 33:101112. https://doi.org/10.1016/j.jwpe.2019.101112
26. Sharma G, Naushad M (2020) Adsorptive removal of noxious cadmium ions from aqueous medium using activated carbon/zirconium oxide composite: isotherm and kinetic modelling. J Mol Liq 310(15):113025. https://doi.org/10.1016/j.molliq.2020.113025
27. Cyganowski P (2020) Synthesis of adsorbents with anion exchange and chelating properties for separation and recovery of precious metals – a review. Solvent Ext Ion Exch 38(2):143–165. https://doi.org/10.1080/07366299.2020.1720117
28. Lee JC, Hong HJ, Chung KW, Kim S (2020) Separation of platinum, palladium and rhodium from aqueous solutions using ion exchange resin: a review. Sep Purif Technol 246:116896. https://doi.org/10.1016/j.seppur.2020.116896
29. Ramohlola KE, Masikini M, Mdluli SB, Monama GR, Hato MJ, Molapo KM, Modibane KD (2017) Electrocatalytic hydrogen production properties of poly (3-aminobenzoic acid) doped with metal organic frameworks. Int J Electrochem Sci 12:4392–4405. https://doi.org/10.20964/2017.05.58
30. Mildan E, Gülfen M (2015) Equilibrium, kinetics, and thermodynamics of Pd(II) adsorption onto poly(m-aminobenzoic acid) chelating polymer. J Appl Polym Sci 132(37):42533. https://doi.org/10.1002/app.42533
31. Wen P, Wang X (2013) Synthesis and visible photocatalytic activities of poly (aminobenzoic acid)/TiO_2 nanocomposites. J Nanomater 2013(795652):1–10. https://doi.org/10.1155/2013/795652
32. Benyoucef A, Huerta F, Vázquez JL, Morallon E (2005) Synthesis and in situ FTIRS characterization of conducting polymers obtained from aminobenzoic acid isomers at platinum electrodes. Eur Polym J 41(4):843–852. https://doi.org/10.1016/j.eurpolymj.2004.10.047
33. Fındık S, Gülfen M, Aydın AO (2014) Adsorption of selenite ions onto poly (1, 8-diaminonaphthalene) synthesized by using ammonium persulfate. Sep Sci Technol 49(18):2890–2896. https://doi.org/10.1080/01496395.2014.946144
34. Akkaya T, Gülfen M, Olgun U (2013) Adsorption of rhodium(III) ions onto poly (1, 8-diaminonaphthalene) chelating polymer: equilibrium, kinetic and thermodynamic study. React Funct Polym 73(12):1589–1596. https://doi.org/10.1016/j.reactfunctpolym.2013.09.001
35. Rivas BL, Sanchez CO (2003) Poly(2-) and (3-aminobenzoic acids) and their copolymers with aniline: synthesis, characterization, and properties. J Appl Polym Sci 89(10):2641–2648. https://doi.org/10.1002/app.12236
36. Fatuch JC, Soto-Oviedo MA, Avellaneda CO, Franco MF, Romão W, De Paoli MA, Nogueira AF (2009) Synthesis and characterization of aniline copolymers containing carboxylic groups and their application as sensitizer and hole conductor in solar cells. Synth Met 159(21–22):2348–2354. https://doi.org/10.1016/j.synthmet.2009.07.038
37. Deng Q, Li Y, Wu J, Liu Y, Fang G, Wang S, Zhang Y (2012) Highly sensitive fluorescent sensing for water based on poly (*m*-aminobenzoic acid). Chem Commun 48(24):3009–3011. https://doi.org/10.1039/C2CC17856G
38. Li XG, Feng H, Huang MR (2009) Strong adsorbability of mercury ions on aniline/sulfoanisidine copolymer nanosorbents. Chem Eur J 15(18):4573–4581. https://doi.org/10.1002/chem.200802431
39. Olgun U, Gülfen M (2014) Doping of poly(o-phenylenediamine): spectroscopy, voltammetry, conductivity and band gap energy. React Funct Polym 77:23–29. https://doi.org/10.1016/j.reactfunctpolym.2014.02.006
40. Rao PS, Sathyanarayana DN (2002) Synthesis of electrically conducting copolymers of aniline with o/m-aminobenzoic acid by an inverse emulsion pathway. Polymer 43(18):5051–5058. https://doi.org/10.1016/S0032-3861(02)00341-5
41. Heydari MH, Zebhi H, Farhadi K, Moghadam PN (2016) Electrochemical synthesis of nanostructure poly (3-aminobenzoic

acid), polyaniline and their bilayers on 430SS and their corrosion protection performances. Synth Met 220(7):78–85. https://doi.org/10.1016/j.synthmet.2016.04.019
42. Kamaraj K, Karpakam V, Sathiyanarayanan S, Venkatachari G (2010) Electrosysnthesis of poly(aniline-co-m-amino benzoic acid) for corrosion protection of steel. Mater Chem Phys 122:123–128. https://doi.org/10.1016/j.matchemphys.2010.02.061
43. McNaught AD, Wilkinson A (1997) IUPAC, Compendium of chemical terminology, 2nd ed. (the Gold Book). Blackwell Scientific Publications, Oxford. https://doi.org/10.1351/goldbook
44. Labib SA, Yousif AM, Ibrahim IA, Atia AA (2018) Adsorption of rhodium by modified mesoporous cellulose/silica sorbents: equilibrium, kinetic, and thermodynamic studies. J Porous Mater 25(2):383–396. https://doi.org/10.1007/s10934-017-0449-3
45. Febrianto J, Kosasih AN, Ju YH, Sunarso J, Indraswati N, Ismandji S (2009) Equilibrium and kinetic studies in adsorption of heavy metals using biosorbent: a summary of recent studies. J Hazard Mater 162:616–645. https://doi.org/10.1016/j.jhazmat.2008.06.042
46. Tofan L, Bunia I, Paduraru C, Teodosiu C (2017) Synthesis, characterization and experimental assessment of a novel functionalized macroporous acrylic copolymer for gold separation from wastewater. Process Saf Environ Prot 106:150–162. https://doi.org/10.1016/j.psep.2017.01.002
47. Suganya S (2018) Influence of ultrasonic waves on preparation of active carbon from coffee waste for the reclamation of effluents containing Cr (VI) ions. J Ind Eng Chem 60:418–430. https://doi.org/10.1016/j.jiec.2017.11.029
48. Basha S, Murthy ZVP (2007) Kinetic and equilibrium models for biosorption of Cr(VI) on chemically modified seaweed, cystoseira indica. Process Biochem 42(11):1521–1529. https://doi.org/10.1016/j.procbio.2007.08.004
49. Shen YF, Xue WY (2007) Recovery palladium, gold and platinum from hydrochloric acid solution using 2-hydroxy-4-sec-octanoyl diphenyl-ketoxime. Sep Purif Technol 56(3):278–283. https://doi.org/10.1016/j.seppur.2007.02.001
50. Erim ÜC, Gülfen M, Aydın AO (2013) Separation of gold (III) ions by 1,8-diaminonaphthalene-formaldehyde chelating polymer. Hydrometallurgy 134:87–95. https://doi.org/10.1016/j.hydromet.2013.02.005
51. Abodif AM, Li M, Sanjrani MA, Ahmed ASA, Belvett N, Wei ZZ, Ning D (2020) Mechanisms and models of adsorption: TiO_2-supported biochar for removal of 3,4-dimethylaniline. ACS Omega 5(23):13630–13640. https://doi.org/10.1021/acsomega.0c00619
52. Hemavathy RV, Kumar PS, Kanmani K, Jahnavi N (2020) Adsorptive separation of Cu(II) ions from aqueous medium using thermally/chemically treated Cassia fistula based biochar. J Clean Prod 249:119390. https://doi.org/10.1016/j.jclepro.2019.119390
53. Kumar PS, Senthamarai C, Sai Deepthi ASL, Bharani R (2013) Adsorption isotherms, kinetics and mechanism of Pb (II) ions removal from aqueous solution using chemically modified agricultural waste. Can J Chem Eng 91(12):1950–1956. https://doi.org/10.1002/cjce.21784
54. Anitha T, Kumar PS, Kumar SK (2015) Binding of Zn (II) ions to chitosan–PVA blend in aqueous environment: adsorption kinetics and equilibrium studies. Environ Prog Sustain Energy 34(1):15–22. https://doi.org/10.1002/ep.11943
55. Wu FC, Tseng RL, Juang RS (2009) Characteristics of Elovich equation used for the analysis of adsorption kinetics in dye-chitosan systems. Chem Eng J 150(2–3):366–373. https://doi.org/10.1016/j.cej.2009.01.014
56. Zhu W, Liu J, Li M (2014) Fundamental studies of novel zwitterionic hybrid membranes: kinetic model and mechanism insights into strontium removal. Sci World J 2014:485820. https://doi.org/10.1155/2014/485820
57. Ngueagni PT, Woumfo ED, Kumar PS, Siéwé M, Vieillard J, Brun N, Nkuigue PF (2020) Adsorption of Cu(II) ions by modified horn core: effect of temperature on adsorbent preparation and extended application in river water. J Mol Liq 298:112023. https://doi.org/10.1016/j.molliq.2019.112023
58. Fujiwara K, Ramesh A, Maki T, Hasegawa H, Ueda K (2007) Adsorption of platinum(IV), palladium (II) and gold (III) from aqueous solutions onto l-lysine modified crosslinked chitosan resin. J Hazard Mater 146(1–2):39–50. https://doi.org/10.1016/j.jhazmat.2006.11.049
59. Park HN, Choi HA, Won SW (2018) Fibrous polyethylenimine/polyvinyl chloride crosslinked adsorbent for the recovery of Pt(IV) from acidic solution: Adsorption, desorption and reuse performances. J Clean Prod 176:360–369. https://doi.org/10.1016/j.jclepro.2017.12.160
60. Hemavathy RRV, Kumar PS, Suganya S, Swetha V, Varjani SJ (2019) Modelling on the removal of toxic metal ions from aquatic system by different surface modified Cassia fistula seeds. Bioresour Technol 281:1–9. https://doi.org/10.1016/j.biortech.2019.02.070
61. Saravanan A, Kumar PS, Renita AA (2018) Hybrid synthesis of novel material through acid modification followed ultrasonication to improve adsorption capacity for zinc removal. J Clean Prod 172:92–105. https://doi.org/10.1016/j.jclepro.2017.10.109
62. Lim CR, Lin S, Yun YS (2020) Highly efficient and acid-resistant metal-organic frameworks of MIL-101 (Cr)-NH2 for Pd (II) and Pt (IV) recovery from acidic solutions: adsorption experiments, spectroscopic analyses, and theoretical computations. J Hazard Mater 387:121689. https://doi.org/10.1016/j.jhazmat.2019.121689
63. Geng Y, Li J, Lu W, Wang N, Xiang Z, Yang Y (2020) Au (III), Pd (II) and Pt (IV) adsorption on amino-functionalized magnetic sorbents: behaviors and cycling separation routines. Chem Eng J 381:122627. https://doi.org/10.1016/j.cej.2019.122627
64. Godlewska-Żyłkiewicz B, Sawicka S, Karpińska J (2019) Removal of platinum and palladium from wastewater by means of biosorption on fungi *Aspergillus* sp. and yeast *saccharomyces* sp. Water 11:1522. https://doi.org/10.3390/w11071522
65. Yousif AM, Labib SA, Ibrahim IA, Atia AA (2019) Recovery of Pt (IV) from aqueous solutions using magnetic functionalized cellulose with quaternary amine. Sep Sci Technol 54(8):1257–1268. https://doi.org/10.1080/01496395.2018.1534866
66. Bediako JK, Park SW, Choi JW, Song MH, Yun YS (2019) High-performance and acid-tolerant polyethylenimine-aminated polyvinyl chloride fibers: fabrication and application for recovery of platinum from acidic wastewaters. J Environ Chem Eng 7(1):102839. https://doi.org/10.1016/j.jece.2018.102839
67. Mosai AK, Chimuka L, Cukrowska EM, Kotzé IA, Tutu H (2019) The recovery of Platinum (IV) from aqueous solutions by hydrazine-functionalised zeolite. Miner Eng 131:304–312. https://doi.org/10.1016/j.mineng.2018.11.028
68. Garole DJ, Choudhary BC, Paul D, Borse AU (2018) Sorption and recovery of platinum from simulated spent catalyst solution and refinery wastewater using chemically modified biomass as a novel sorbent. Environ Sci Pollut Res 25(11):10911–10925. https://doi.org/10.1007/s11356-018-1351-5
69. Anbia M, Rahimi F (2017) Adsorption of platinum (IV) from an aqueous solution with magnetic cellulose functionalized with thiol and amine as a nano-active adsorbent. J Appl Polym Sci 134(39):45361. https://doi.org/10.1002/app.45361